Quasi-phase-matching engineering for spatial control of entangled two-photon states

Juan P. Torres, Adrian Alexandrescu, Silvia Carrasco, and Lluis Torner

ICFO–Institut de Ciencies Fotoniques, and Department of Signal Theory and Communications, Universitat Politecnica de Catalunya, 08034 Barcelona, Spain

Received August 21, 2003

We show that transverse engineering of quasi-phase-matched geometries can be used to tailor the spatial mode function that describes the quantum state of photon pairs generated in spontaneous parametric down-conversion. We study several geometries and reveal how properly engineered gratings affect, in particular, the spatial correlations embedded in two-photon entangled states. © 2004 Optical Society of America

OCIS codes: 270.5290, 190.4410.

Spontaneous parametric downconversion is a reliable source of photons with entangled properties. The two-photon states that it generates exhibit spatial entanglement embedded in the corresponding mode function, thus yielding entanglement in an infinite-dimensional Hilbert space. For example, the spatial structure of the mode functions of entangled signal and idler photons forms the basis of multidimensional quantum imaging[1–3] or can be used to increase the efficiency of multidimensional quantum communication protocols. Thus, controlling the spatial characteristics of photons is an issue of paramount importance. In some cases, such a goal can be achieved by manipulation of the properties of the light beam that pumps the downconverting crystal.[1,4] Here we add a new strategy to the toolkit, which is based on the proper preparation of the downconverting crystal, namely, on spatial quantum-state manipulation by quasi-phase-matching engineering.

Quasi-phase matching is a major alternative to conventional phase matching in many current applications of optical parametric processes.[5] In quantum optics, counterpropagating entangled photons generated in homogeneous quasi-phase-matched (QPM) waveguides have been shown to generate tunable frequency entanglement with a largely reduced bandwidth.[6] Moreover, waveguide modes have been shown to provide new means to control the spatial characteristics of photons.[7] However, one of the key properties of quasi-phase matching is its potential to tailor the effective phase matching in the form of complex geometries. Thus, longitudinal modulation of the nonlinearity has been shown to strongly affect the spatiotemporal properties of entangled photon pairs.[8] Here we introduce a scheme that allows the spatial mode function of the two-photon state to be controlled by making use of transversely patterned QPM gratings. The scheme is valid in both bulk and waveguide configurations and in photonic crystal geometries. Such QPM patterns are used in classical nonlinear optics, e.g., for beam shaping in parametric processes[9–11] and in spatial soliton switching.[12] Transverse patterning of QPM gratings might be more convenient than the direct manipulation of the pump light beam mentioned above when large mode function variations are required over small spatial scales or when several functions are to be integrated (and, e.g., cascaded) in a single compact structure.

Let a quadratic nonlinear crystal of length L be illuminated by a laser pump beam propagating in the z direction. The pump beam writes $E_p(\mathbf{x},z,t) = \int \mathrm{d}\mathbf{q} E_0(\mathbf{q}) \exp[ik_p(\mathbf{q})z + i\mathbf{q}\cdot\mathbf{x} - i\omega_p t] + \text{c.c.}$, where ω_p is the angular frequency of the pump beam, $k_p(\mathbf{q}) = [(\omega_s n_p/c)^2 - |\mathbf{q}|^2]^{1/2}$ is the wave number inside the crystal, $\mathbf{q}$ is the transverse spatial frequency, $\mathbf{x} = (x,y)$ is a position in the transverse plane, n_p is the refractive index at the pump wavelength, and $E_0(\mathbf{q})$ is the field profile of the pump beam. The signal and idler photons are assumed to be monochromatic, with $\omega_p = \omega_s + \omega_i$, where ω_s and ω_i are the frequencies of the signal and the idler photons, respectively. This assumption is justified by the use of narrowband interference filters in front of the detectors. Notwithstanding, we have verified that the main conclusions of this Letter also hold when one is considering narrow biphoton bandwidths.

The modulation of the quadratic nonlinearity is described by the function $d(x,z)$. This function can be expressed as the Fourier series[12]

$$d(z,x) = \sum_{n=-\infty}^{\infty} d_n \exp\{in(2\pi/\Lambda)[z - \Phi(x)]\}, \qquad (1)$$

where Λ is the period of the modulation in z, and d_n are the Fourier coefficients of the modulation function. The function $\Phi(x)$ describes the nonuniform transverse pattern. In Fig. 1 we show two examples of transversely patterned QPM gratings. Figure 1(b) corresponds to a parabolic phase profile with $\Phi(x) = \Lambda x^2/(2\lambda_p f)$, where $\lambda_p = 2\pi c/\omega_p$ and f is the equivalent focal length of the grating at the pump wavelength.[11] Figure 1(c) corresponds to a dislocation configuration, where $\Phi(x)$ take values 0 and $\Lambda/2$ with transverse period G. For comparison, Fig. 1(a) shows a QPM grating with no transverse pattern. In the usual configurations, only the mode of the expansion of $d(x,z)$ that fulfills the phase-matching condition contributes significantly to the nonlinear process. The two-photon quantum state that is generated is given by[13]

$$|\Psi\rangle = \int \mathrm{d}\mathbf{q}_s \mathrm{d}\mathbf{q}_i \Phi(\mathbf{q}_s,\mathbf{q}_i) a_s^{\dagger}(\mathbf{q}_s) a_i^{\dagger}(\mathbf{q}_i) |0,0\rangle, \qquad (2)$$

0146-9592/04/040376-03$15.00/0

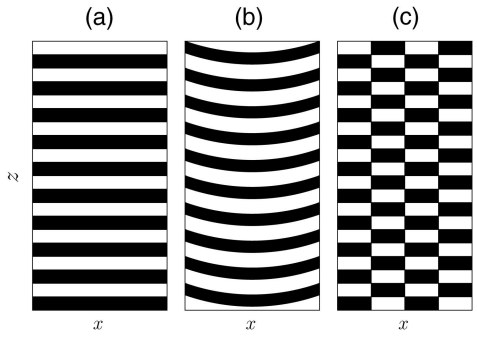

Fig. 1. Diagram of three QPM structures: (a) standard, (b) parabolic, and (c) with multiple dislocations.

where the mode function $\Phi(\mathbf{q}_s, \mathbf{q}_i)$ can be written as

$$\Phi(\mathbf{q}_s, \mathbf{q}_i) = \int \mathrm{d}\mathbf{q}_p E_0(\mathbf{q}_p)\mathrm{d}(\mathbf{q}_s + \mathbf{q}_i - \mathbf{q}_p)W(\mathbf{q}_p, \mathbf{q}_s, \mathbf{q}_i)\,. \tag{3}$$

The expression for the function $\mathrm{d}(\mathbf{q})$ is related to the specific form of the transverse pattern of the grating, i.e., $\mathrm{d}(\mathbf{q}) = \int \mathrm{d}\mathbf{x}\mathrm{d}(\mathbf{x})\exp(-i\mathbf{q}\cdot\mathbf{x})$, where $\mathrm{d}(\mathbf{x}) = \exp[i2\pi\Phi(\mathbf{x})/\Lambda]$ designates the transverse pattern of the grating. The function $W(\mathbf{q}_p, \mathbf{q}_s, \mathbf{q}_i)$, which comes from the phase-matching condition in the longitudinal direction, is given by

$$W(\mathbf{q}_p, \mathbf{q}_s, \mathbf{q}_i) = \mathrm{sinc}(\Delta kL/2)\exp(-i\Delta kL/2)\,, \tag{4}$$

where $\Delta k = k_p(\mathbf{q}_p) - k_s(\mathbf{q}_s) - k_i(\mathbf{q}_i) - 2\pi/\Lambda$, $k_s(\mathbf{q}_s) = [(\omega_s n_s/c)^2 - |\mathbf{q}_s|^2]^{1/2}$ and $k_i(\mathbf{q}_i) = [(\omega_i n_i/c)^2 - |\mathbf{q}_i|^2]^{1/2}$, where n_s and n_i are the refractive indices at the signal and idler wavelengths, respectively, inside the crystal. Normalization of the state requires that $\int \mathrm{d}\mathbf{q}_s \mathrm{d}\mathbf{q}_i |\Phi(\mathbf{q}_s, \mathbf{q}_i)|^2 = 1$. The signal and idler photons traverse linear optical systems described by transfer functions $H_s(\mathbf{x}_1, z_1, \mathbf{q}_s)$ and $H_i(\mathbf{x}_2, z_2, \mathbf{q}_i)$, respectively. The probability amplitude is thus given by[2]

$$\begin{aligned} A(\mathbf{x}_1, z_1, t_1; \mathbf{x}_2, z_2, t_2) = &\int \mathrm{d}\mathbf{q}_s \mathrm{d}\mathbf{q}_i \Phi(\mathbf{q}_s, \mathbf{q}_i) \\ &\times H_s(\mathbf{x}_1, z_1, \mathbf{q}_s) H_i(\mathbf{x}_2, z_2, \mathbf{q}_i) \\ &\times \exp(-i\omega_s t_1 - i\omega_i t_2)\,. \end{aligned} \tag{5}$$

The biphoton rate, i.e., the probability of coincidence of photons at positions $(\mathbf{x}_1, z_1)$ and $(\mathbf{x}_2, z_2)$, is given by $G(\mathbf{x}_1, z_1; \mathbf{x}_2, z_2) = |A(\mathbf{x}_1, z_1, t_1; \mathbf{x}_2, z_2, t_2)|^2$. A special correlation function that we use throughout this Letter to show the spatial characteristics of the photons is the conditional coincidence rate $I_0(\mathbf{x}_1) = G(\mathbf{x}_1, \mathbf{x}_2 = 0)$, which is proportional to the probability of detecting a photon at $(\mathbf{x}_1, z_1)$ when a photon is detected at $\mathbf{x}_2 = 0$. In this scheme, the signal and idler photons produced by the nonlinear crystal pass through identical 2-f optical systems, with focal lengths $f_s = f_i$, whose transfer function for the signal photon is given by $H_s(\mathbf{x}_1, z_1, \mathbf{q}_s) \sim \delta[\mathbf{q}_s - 2\pi x_1/(\lambda_s f_s)]$, and similarly for the idler photon. The observation planes are assumed to be located at the focal length of the lens, $z_1 = z_2 = f_s$. The probability amplitude can now be written as

$$\begin{aligned} A(\mathbf{x}_1, z_1 = f_s, t_1; \mathbf{x}_2, z_2 = f_s, t_2) = &\left(\frac{2\pi}{\lambda_s f_s}\right)^2 \\ &\times \Phi\left(\frac{2\pi\mathbf{x}_1}{\lambda_s f_s}, \frac{2\pi\mathbf{x}_2}{\lambda_s f_s}\right)\exp(-i\omega_s t_1 + i\omega_i t_2)\,. \end{aligned} \tag{6}$$

The 2-f system provides a spatial image of the mode function of the two-photon state $\Phi(\mathbf{q}_s, \mathbf{q}_i)$, so by measuring the coincidence rates at different positions in the transverse plane one obtains information about the shape of the mode function.

Figure 2 shows the conditional coincidence rate predicted for a parabolic phase grating [Fig. 1(b)]. The shape of the transverse pattern in the spatial frequency domain is written as $\mathrm{d}(\mathbf{q}) \sim \exp[-i\lambda_p f/(4\pi)\,|\mathbf{q}|^2]$. In Fig. 2(b) the equivalent focal length is $f = 4$ cm, and in Fig. 2(c) it is $f = 2$ cm. For comparison, we show in Fig. 2(a) a grating with no transverse pattern. The effect of the parabolic phase grating is to create an elliptical mode function, with the ellipticity increasing with the inverse of the focal length. For free-space propagation of the signal and idler photons in the paraxial approximation, i.e., $H_s(\mathbf{x}_1, z_1, \mathbf{q}_s) \sim \exp(-i|\mathbf{q}_s|^2/(2k_s) + i\mathbf{q}_s \cdot x_1 + ik_s z_1)$, and similarly for the idler photon, this yields that the conditional coincidence rate function will focus in the x direction at $z_1 = f$. The main result shown in Fig. 2 is that the parabolic QPM grating can be used to shape the biphoton rate. Thus the QPM grating behaves effectively as a cylindrical lens for the generation of the two-photon state, hence producing the quantum version of the classical result.[11]

Engineered QPM patterns offer promising possibilities for tailoring the spatial shape of the probability amplitude such that the correlations between the output photons can be strongly manipulated. The transverse pattern shown in Fig. 1(c) can be decomposed into a Fourier series, i.e., $d(x) = \sum_n C_n \exp(i2\pi n/G)$ for $n = \ldots -3, -1, 1, 3\ldots$, where G is the transverse spatial period of the grating and $C_n = 2/(in\pi)$. The conditional coincidence rate can be written as

$$\begin{aligned} I_0(\mathbf{x}_1) \sim \Bigg| &\sum_n C_n E_0\left(\frac{2\pi\mathbf{x}_1}{\lambda_s f_s} - \frac{2\pi n}{G}\right) \\ &\times W\left(\frac{2\pi\mathbf{x}_1}{\lambda_s f_s} - \frac{2\pi n}{G}, \frac{2\pi\mathbf{x}_1}{\lambda_s f_s}, 0\right)\Bigg|^2 . \end{aligned} \tag{7}$$

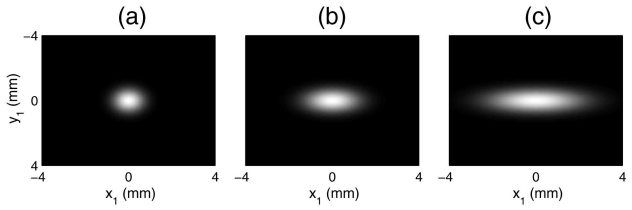

Fig. 2. Conditional coincidence rate $I_0(\mathbf{x}_1, z_1)$ for a parabolic phase grating. (a) QPM with no transverse pattern; (b), (c) parabolic phase gratings with equivalent focal lengths $f = 4$ cm and $f = 2$ cm, respectively. Conditions: crystal length, $L = 1$ mm; beam width of the pump beam, $w_0 = 100$ μm; focal length of the 2-f system, $f_s = 20$ cm; pump wavelength, $\lambda_p = 532$ nm; signal and idler wavelengths, $\lambda_s = \lambda_i = 1064$ nm.

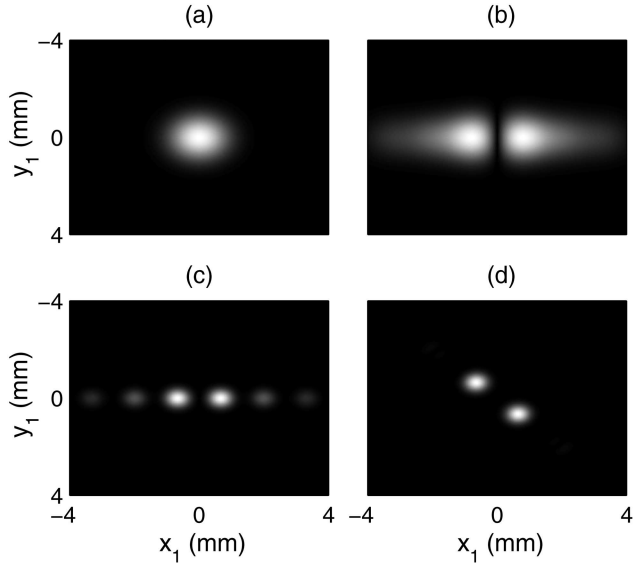

Fig. 3. Conditional coincidence rate $I_0(\mathbf{x}_1, z_1)$ for the multiple dislocation transverse grating with transverse period $G = 80\ \mu$m. (a) $w_0 = 20\ \mu$m, $L = 0.1$ mm, QPM with no transverse pattern; (b) $w_0 = 20\ \mu$m, $L = 0.1$ mm, transverse pattern in the x dimension; (c) $w_0 = 50\ \mu$m, $L = 0.1$ mm, transverse pattern in the x dimension; (d) $w_0 = 50\ \mu$m, $L = 1$ mm, transverse pattern in the x and y dimensions. Conditions: focal length of the 2-f system, $f_s = 5$ cm; pump wavelength, $\lambda_p = 532$ nm; signal and idler wavelengths, $\lambda_s = \lambda_i = 1064$ nm.

In the thin crystal approximation the effect of each term of the decomposition given in relation (7) is to shift the pump beam function to the position $x_n = n\lambda_s f_s/G$, modulated by its corresponding amplitude in the Fourier decomposition. When the crystal length is increased, the phase-matching function W acts as a spatial filter whose effects cannot be ignored.[2] In Figs. 3(b) and 3(c) we plot the conditional coincidence rate for the transverse pattern shown in Fig. 1(c) with period $G = 80\ \mu$m and crystal length $L = 0.1$ mm. For comparison, we show in Fig. 3(a) the function $I_0(\mathbf{x}_1)$ for a grating with no transverse pattern. For beam width $w_0 = 20\ \mu$m, the pump beam cannot experience the full transverse modulation of the nonlinear coefficient, so the nonlinearity effectively behaves as a single dislocation. The peaks of the expression given by relation (7) are separated, $2\lambda_s f_s/G$, whereas the width of each one is $\sim\lambda_s f_s/(4W)$; thus Fig. 3(b) does not show a multipeak structure for $I_0(x_1)$. For larger values of the beam width there are more dislocations inside the width of the pump beam, so the conditional coincidence rate has the form of a sinc function. Increasing the crystal length to $L = 1$ mm causes the secondary peaks that one can observe in Fig. 3(c) to disappear because of the spatial filtering effect of the longitudinal phase matching. Naturally, more-complex QPM structures than those considered here yield more-complex spatial shapes of the spatial amplitude of the two-photon state.

The scheme put forward here applies also to nonlinear photonic crystals, i.e., to nonlinear crystals with modulation of the nonlinearity in two and three dimensions,[14] which offer fascinating opportunities for the manipulation of light. In Fig. 3(d) we plot the function $I_0(\mathbf{x}_1)$ for a nonlinear photonic crystal with the same modulation of the nonlinear coefficient in both the x and the y dimensions and crystal length $L = 1$ mm.

In conclusion, we have shown that properly designed transversely varying QPM gratings allow tailoring the spatial mode function of the two-photon state generated in spontaneous parametric downconversion, which results in large modifications of the spatial correlations between the photons. We note that QPM engineering also modifies the multimodal coherent superposition of orbital angular momenta that consist of the two-photon states,[15–18] thus providing a powerful way to control the effective finite Hilbert space where the corresponding multidimensional entanglement takes place.[19]

This research was supported by the Generalitat de Catalunya and by the Spanish government through grant BFM2002-2861. J. P. Torres's e-mail address is jperez@tsc.upc.es.

References

1. T. B. Pittman, D. V. Strekalov, D. N. Klyshko, M. H. Rubin, A. V. Sergienko, and Y. H. Shih, Phys. Rev. A **53,** 2804 (1996).
2. A. F. Abouraddy, B. E. A. Saleh, A. V. Sergienko, and M. C. Teich, J. Opt. Soc. Am. B **19,** 1174 (2002).
3. A. Gatti, E. Brambilla, and L. A. Lugiato, Phys. Rev. Lett. **90,** 133603 (2003).
4. C. H. Monken, P. H. Souto Ribeiro, and S. Padua, Phys. Rev. A **57,** 3123 (1998).
5. M. M. Fejer, G. A. Magel, D. H. Jundt, and R. L. Byer, IEEE J. Quantum Electron. **28,** 2631 (1992).
6. M. C. Booth, M. Atature, G. Di Giuseppe, B. E. A. Saleh, A. V. Sergienko, and M. C. Teich, Phys. Rev. A **66,** 023815 (2002).
7. K. Banaszek, A. B. U'Rem, and I. A. Walmsley, Opt. Lett. **26,** 1367 (2001).
8. G. Di Giuseppe, M. Atature, M. D. Shaw, A. V. Sergienko, B. E. A. Saleh, and M. C. Teich, Phys. Rev. A **66,** 013801 (2002).
9. P. E. Powers, T. J. Kulp, and S. E. Bisson, Opt. Lett. **23,** 159 (1998).
10. G. Imeshev, M. Proctor, and M. M. Fejer, Opt. Lett. **23,** 673 (1998).
11. J. R. Kurz, A. M. Schober, D. S. Hum, A. J. Saltzman, and M. M. Fejer, IEEE J. Sel. Top. Quantum Electron. **8,** 660 (2002).
12. C. B. Clausen and L. Torner, Opt. Lett. **24,** 7 (1999).
13. B. E. A. Saleh, A. F. Abouraddy, A. V. Sergienko, and M. C. Teich, Phys. Rev. A **62,** 043816 (2000).
14. V. Berger, Phys. Rev. Lett. **81,** 4136 (1998).
15. A. Mair, A. Vaziri, G. Weihs, and A. Zeilinger, Nature **412,** 313 (2001).
16. G. Molina-Terriza, J. P. Torres, and L. Torner, Phys. Rev. Lett. **88,** 013601 (2002).
17. S. Franke-Arnold, S. M. Barnett, M. J. Padgett, and L. Allen, Phys. Rev. A **65,** 033823 (2002).
18. J. P. Torres, Y. Deyanova, L. Torner, and G. Molina-Terriza, Phys. Rev. A **67,** 052313 (2003).
19. C. K. Law, I. A. Walmsley, and J. H. Eberly, Phys. Rev. Lett. **84,** 5304 (2000).